Int. J. Electron. Commun. (AEÜ) 166 (2023) 154652

Contents lists available at ScienceDirect

International Journal of Electronics and Communications

journal homepage: www.elsevier.com/locate/aeue

Regular paper

Photonic controlled metasurface for intelligent antenna beam steering applications including 6G mobile communication systems

Zainab S. Muqdad [a], Mohammad Alibakhshikenari [b,*], Taha A. Elwi [c,d,*], Zaid A. Abdul Hassain [a], Bal.S. Virdee [e], Richa Sharma [e], Salahuddin Khan [f], Nurhan Türker Tokan [g], Patrizia Livreri [h], Francisco Falcone [i,j], Ernesto Limiti [k]

[a] Department of Electrical Engineering, Mustansiriyah University, Baghdad, Iraq
[b] Department of Signal Theory and Communications, Universidad Carlos III de Madrid, 28911 Leganés, Madrid, Spain
[c] Department of Communication Engineering, Al-Ma'moon University College, Baghdad, Iraq
[d] International Applied and Theoretical Research Center (IATRC), Baghdad Quarter, Iraq
[e] Center for Communications Technology, London Metropolitan University, UK
[f] College of Engineering, King Saud University, P.O.Box 800, Riyadh 11421, Saudi Arabia
[g] Department of Electronics and Communications Engineering, Yildiz Technical University, Esenler, Istanbul 34220, Turkey
[h] Department of Engineering, University of Palermo, viale delle Scienze BLDG 9, Palermo, IT 90128, Sicily, Italy
[i] Electric, Electronic and Communication Engineering Department, and Institute of Smart Cities, Public University of Navarre, 31006 Pamplona, Spain
[j] School of Engineering and Sciences, Tecnologico de Monterrey, Monterrey 64849, Mexico
[k] Electronic Engineering Department, University of Rome "Tor Vergata", Via del Politecnico 1, 00133, Rome, Italy

ARTICLE INFO

Keywords:
Reconfigurable devices
Metasurface
Photonic systems
Fractal geometries
Patch antenna
Beam steering

ABSTRACT

This paper presents a novel metasurface antenna whose radiation characteristics can be remotely controlled by optical means using PIN photodiodes. The proposed reconfigurable antenna is implemented using a single radiating element to minimize the size and complexity. The antenna is shown to exhibit a large impedance bandwidth and is capable of radiating energy in a specified direction. The proposed antenna consists of a standard rectangular patch on which is embedded an H-tree shaped fractal slot of order 3. The fractal slot is used to effectively reduce the physical size of the patch by 75 % and to enhance its impedance bandwidth. A metasurface layer is strategically placed above the patch radiator with a narrow air gap between the two. The metasurface layer is a lattice pattern of square framed rhombus ring shaped unit-cells that are interconnected by PIN photodiodes. The metasurface layer essentially acts like a superstrate when exposed to RF/microwave radiation. Placed below the patch antenna is a conductive layer that acts like a reflector to enhance the front-to-back ratio by blocking radiation from the backside of the patch radiator. The patch's main beam can be precisely controlled by photonically illuminating the metasurface layer. The antenna's performance was modelled and analyzed with a commercial 3D electromagnetic solver. The antenna was fabricated on a standard dielectric substrate FR4 and has dimensions of $0.778\lambda_o \times 0.778\lambda_o \times 0.25\lambda_o$ mm^3, where λ_o is the wavelength of free space centered at 1.35 GHz. Measured results confirm the antenna's performance. The antenna exhibits a wide fractional band of 55.5 % from 0.978 to 1.73 GHz for reflection-coefficient (S_{11}) better than −10 dB. It has a maximum gain of 9 dBi at 1.35 GHz with a maximum front-to-back ratio (F/B) of 21 dBi. The main beam can be steered in the elevation plane from −24° to +24°. The advantage of the proposed antenna is it does not require any mechanical movements or complicated electronic systems.

1. Introduction

In recent years, reconfigurable antennas have received great attention [1]. This is a result of their attractive features, such as beam steering, polarization diversity, and multi-band functionality [2]. Reconfigurable antenna can reduce the number of antennas needed in

* Corresponding authors at: Department of Signal Theory and Communications, Universidad Carlos III de Madrid, 28911 Leganés, Madrid, Spain (M. Alibakhshikenari); Department of Communication Engineering, Al-Ma'moon University College, Baghdad, Iraq (T.A. Elwi).
E-mail addresses: mohammad.alibakhshikenari@uc3m.es (M. Alibakhshikenari), tahaelwi82@almamonuc.edu.iq (T.A. Elwi).

https://doi.org/10.1016/j.aeue.2023.154652
Received 31 January 2023; Accepted 30 March 2023
Available online 20 April 2023

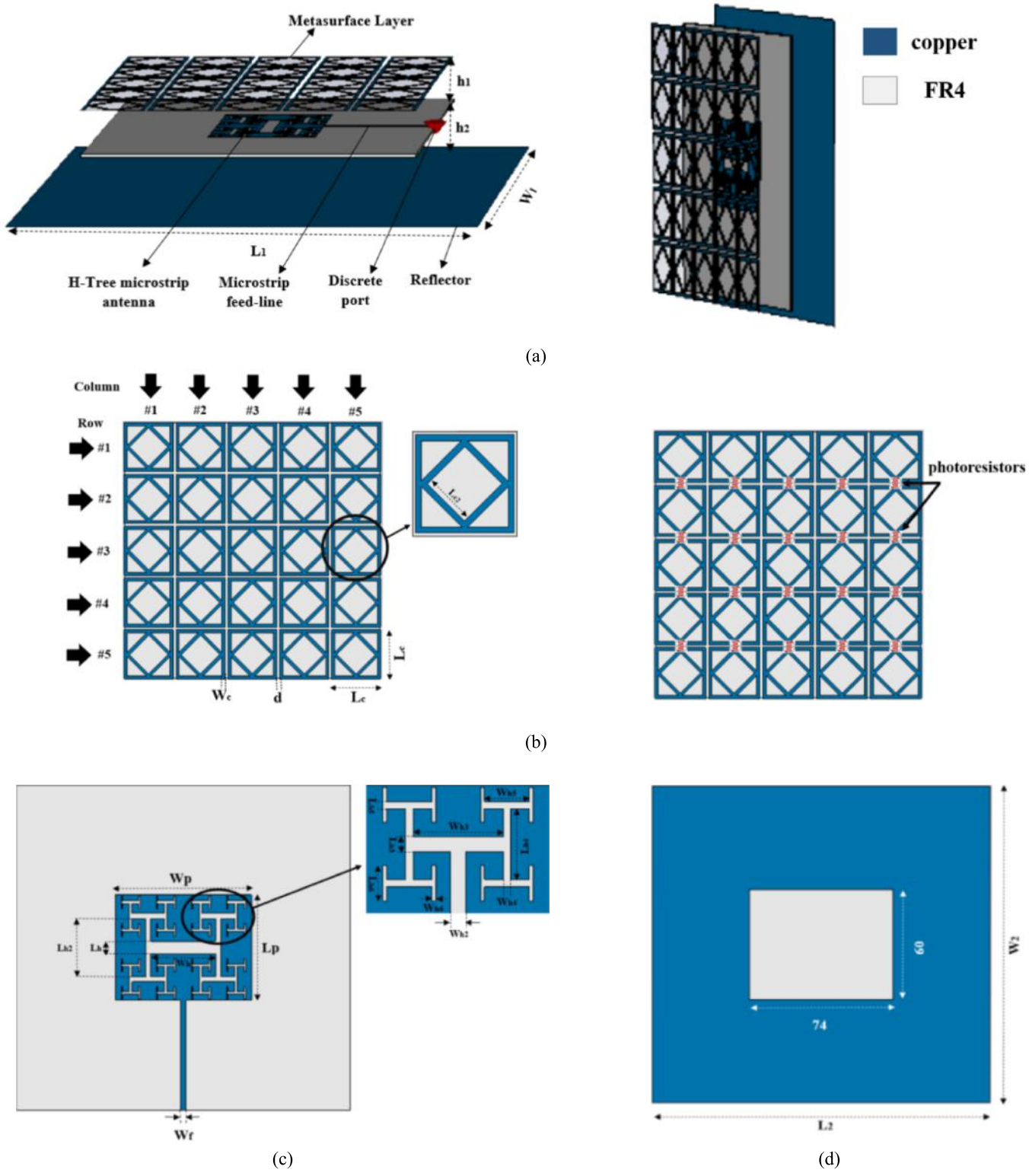

Fig. 1. Structure and geometry of the proposed antenna: (a) isometric view, (b) metasurface layer, (c) antenna patch, and (d) ground plane of patch antenna.

wireless systems thus reducing the overall system size and complexity [3]. The need for such antennas is growing in demand especially for application in smart wireless systems [4]. Because reconfigurable antennas can serve multiple devices, they are a topic of intense research for use as intelligent surfaces in future generation of mobile wireless communication systems like 6G [5].

Several electronically beam-steering antennas proposed recently include Butler matrix [6], phased array [7], Lunburg Lens [8], parallel plate lens [9], Rotman Lens [10], partial reflective surfaces (PRS) [11], and reconfigurable metasurface [12]. Butler matrix antenna reported in [6] provides low-loss and wide bandwidth. While, in [7], a phased array antenna exhibits good radiation performance and rapid beam scanning capability. These two antennas employ multiple radiating elements that make them bulky, and their complexity makes them challenging to

Table 1
Dimensions of the proposed antenna.

Parameter	Dimensions (mm)	Parameter	Dimensions (mm)
$W_1 = L_1$	193	W_{h2}	2.8
$W_2 = L_2$	173	L_{h2}	30.8
W_p	70.7	W_{h3}	16.8
L_p	56	L_{h3}	2.8
h_1	30	W_{h4}	1.4
h_2	25	L_{h4}	13.3
W_c	2	W_{h5}	8.4
L_c	33	L_{h5}	1.4
L_{c2}	15.5	W_{h6}	0.7
d	2	L_{h6}	6.65
W_h	33.6	W_f	2.971
L_h	3.5		

design. Antennas based on Lunburg Lens, parallel plate lens, and Rotman lens, [8]–[10] are capable of steering multiple beams however these antennas are expensive to fabricate. The design of these antennas at the low microwave frequencies makes them bulky [10]. Although reconfigurable PRS can also be used for multi-beam applications however the large profile of this type of antenna makes them unsuitable for many applications [11,12]. Currently, research is focused on designing electronically steerable antennas that can overcome the issues described above [13].

Antenna performance can be controlled using various methods based on mechanical, optical, or electronic. Smart material have also been reported to dynamically reconfigure antenna's radiation characteristics [14]. Most reconfigurable antennas use electronic switches because they can easily be integrated with RF/microwave circuitry. The switching devices commonly used include PIN diodes, RF micro-electromechanical systems (MEMS), varactor diodes, and piezoelectric actuators [2,15–17]. Although, these switches consume low power and have excellent miniaturization factor however they require DC biasing circuitry [14,15]. Also, the operational bandwidth of reconfigurable antennas using varactor diodes is limited [2]. The antennas based on piezoelectric actuators are limited to certain applications due to the effects of the mechanical vibration on the antenna performance [16]. This makes reconfigurable antennas using PIN diodes the default option [17]. DC biasing circuitry of PIN diodes however can adversely interfere with the antenna's performance [18].

Proposed in this paper is an antenna that overcomes the limitations of the existing beam steering techniques. The proposed antenna is based on metasurface and its main beam is reconfigured by photonic means. The antenna uses a single rectangular patch on which is constructed H-tree shaped fractal slot. Placed above the patch is a metasurface layer

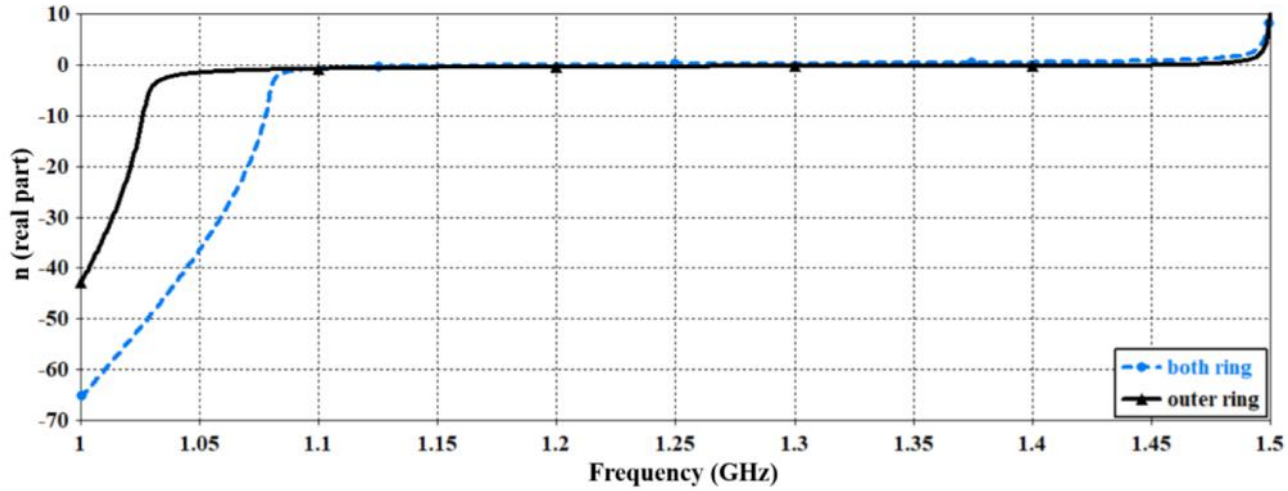

(a)

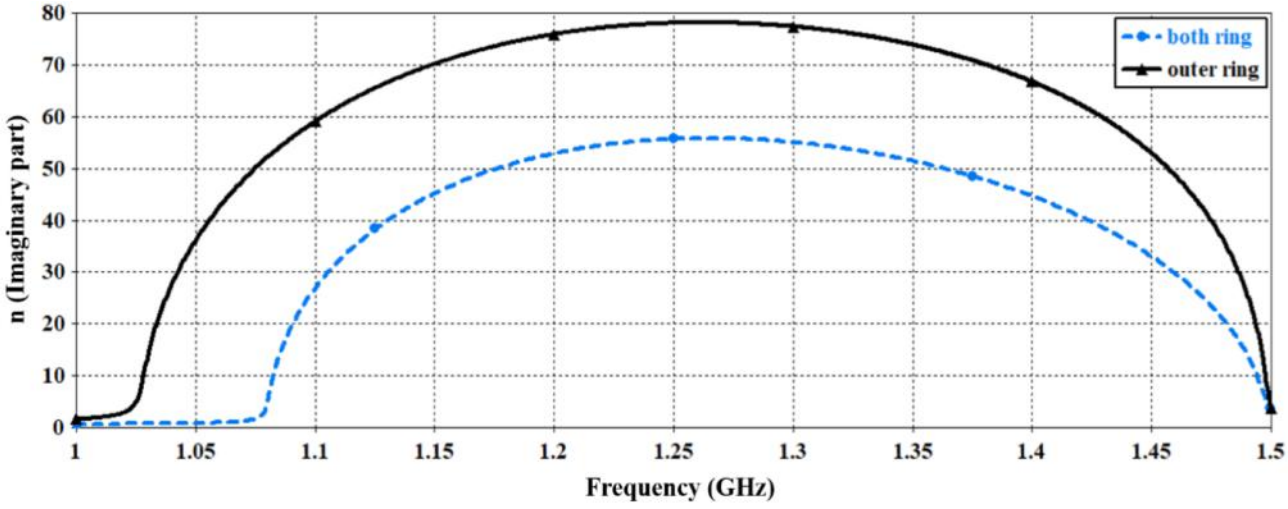

(b)

Fig. 2. Refractive index of the proposed unit cell: (a) Real part, and (b) Imaginary part.

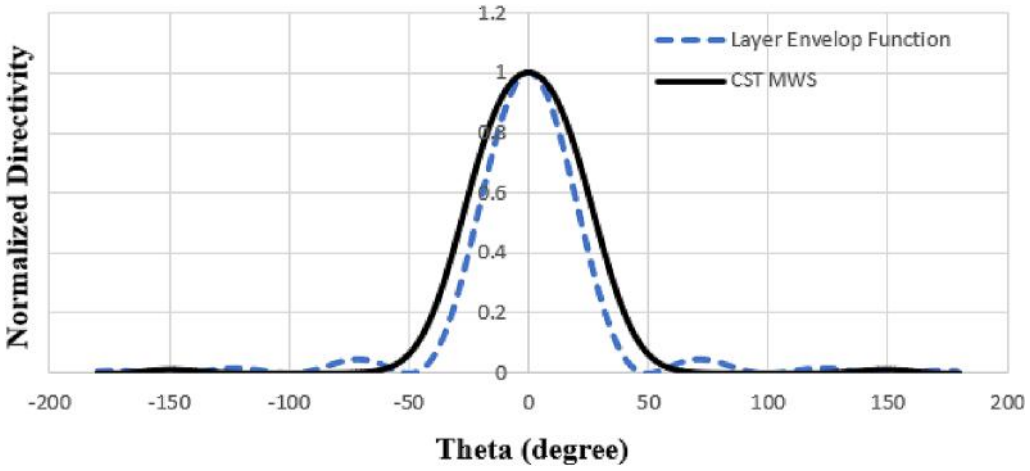

Fig 3. Normalized directivity obtained from Eqn.(2) and CST MWS.

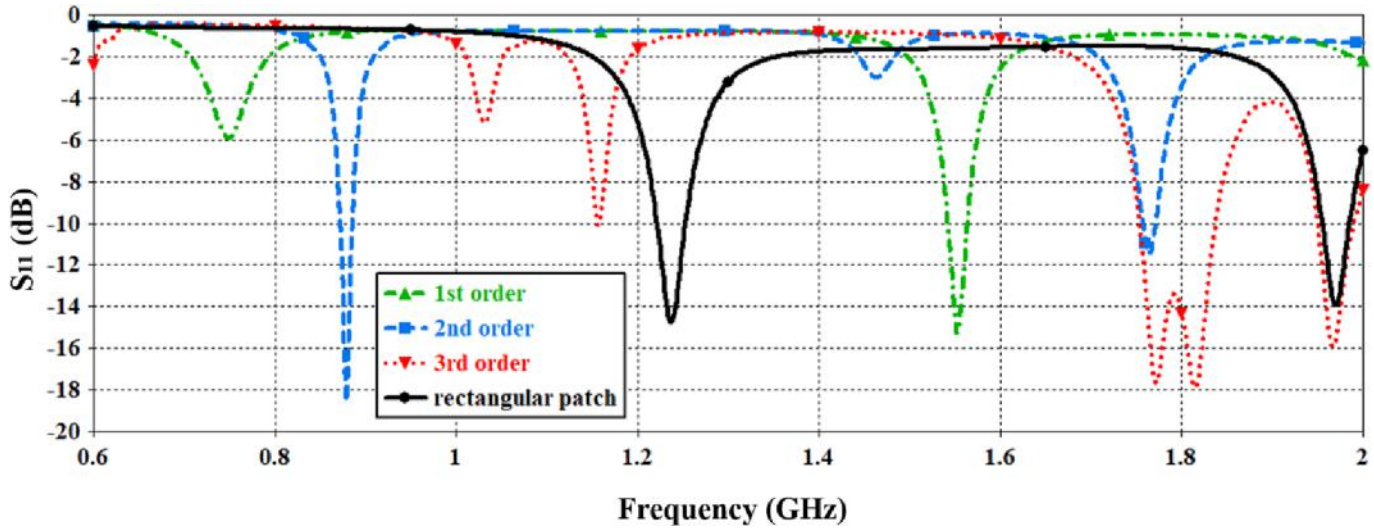

Fig. 4. Simulated S_{11} response of the rectangular patch antenna and the patch antenna loaded with H-Tree slotted fractals of orders 1 to 3.

comprising PIN photodiodes. Placed under the patch is a reflective surface that blocks radiation from the backside of the patch, which is necessary to improve the antenna's front-to-back ratio. Beam steering is implemented by affecting the properties of the metasurface layer. This is achieved by optically switching the array of PIN photodiodes embedded in metasurface layer. By strategically activating the column of PIN photodiodes the main beam of the antenna can be steered by $\pm 24^{\circ}$ in the elevation plane. Moreover, the proposed antenna has a fractional bandwidth of 55.5 % from 0.978 −1.73 GHz.

2. Antenna geometry

The proposed antenna is constructed from a single rectangular patch that is defected with a fractal slot geometry based on a 3rd order H-tree structure, as shown in Fig. 1. High order fractals essentially increase the surface current paths that lowers the resonance frequency of the antenna. This property is exploited here to reduce the electrical dimensions of the patch [19–21]. A rectangular slot is etched on the ground plane of the patch antenna. The purpose of this was to mitigate capacitive coupling between the patch slots with the ground plane which would otherwise trap RF energy and thereby degrade the antenna's gain and radiation efficiency performance [22,23]. A metasurface layer is located on the top of the patch antenna with a narrow air gap between the two. The layer is made of a lattice pattern comprising 5 × 5 matrix of square framed rhombus ring shaped unit-cells where the unit-cells are interconnected by PIN photodiodes. Placed under the patch antenna is a conductive reflector to block backside radiation from the patch antenna. The antenna patch structure is printed on an FR4 substrate of 1.6 mm thickness. The gap between the patch and the reflection layer is made to avoid total internal reflection at the critical angle of wave incidence [24]. The patch antenna is excited through a 50 Ω microstrip line. The dimensions of the proposed antenna are 173 × 173 × 56.6 mm^3. Other geometrical details are listed in Table 1.

3. Metasurface unit-cell

3.1. Unit cell performance

The metasurface layer is constructed from a lattice pattern of unit-cells that consist of a square framed rhombus ring, as shown in Fig. 1 (b). The unit-cell is essentially constructed from two different sized square rings one of which is inside the other. The smaller square ring is oriented by 45° with respect to the larger ring and its size is such that its corners touch the outer ring. This ensures the unit cell is polarization independent and is insensitive to the angle of incidence wave [25]. The inductive and capacitive energy storage by this unit-cell structure is reduced. The metasurface layer comprises a matrix of 5 × 5 unit-cells. The length and width of each unit-cell is approximately λ/8 at 1.13

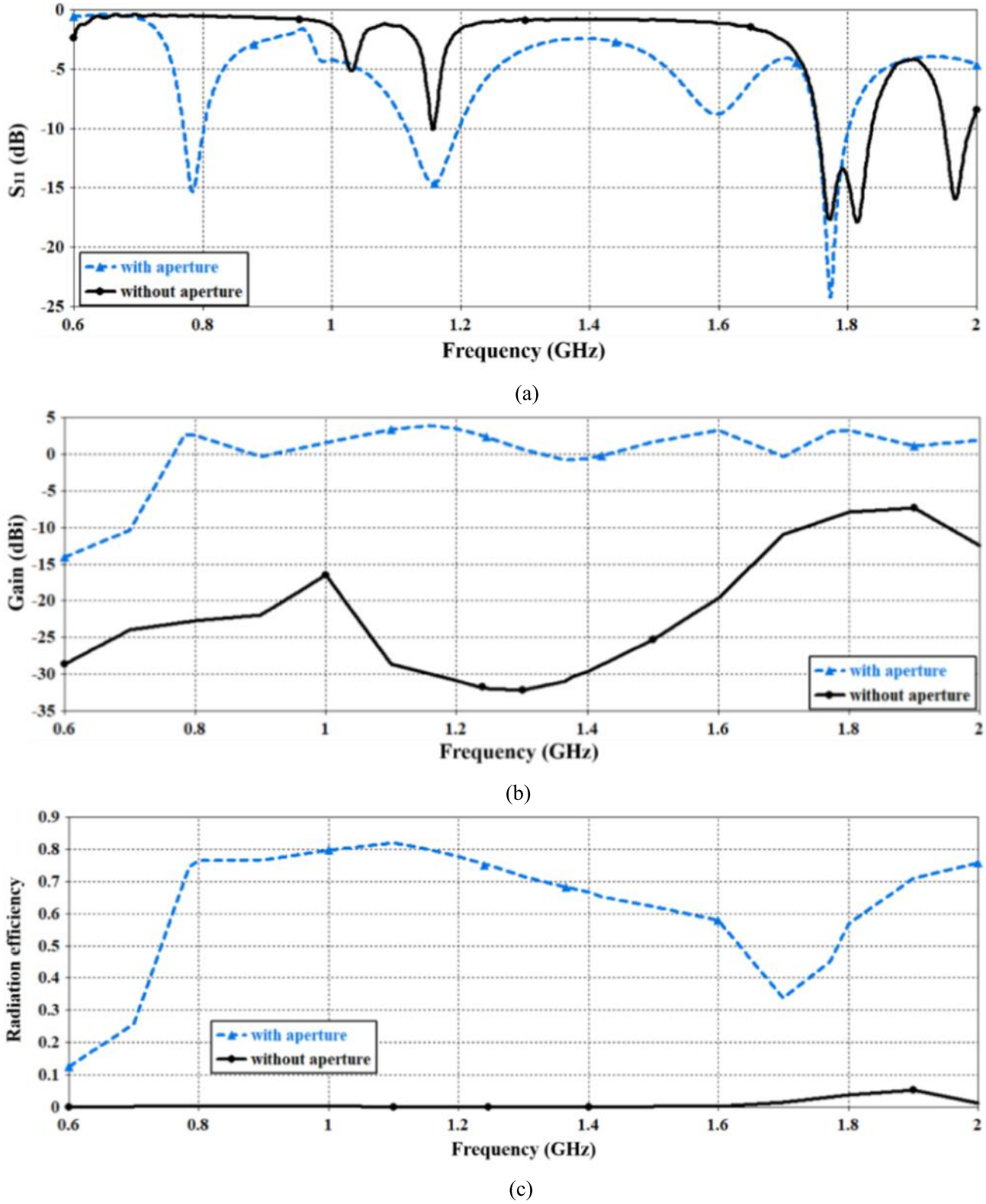

Fig. 5. The comparison of the microstrip patch antenna with and without the ground plane aperture: (a) S_{11}, (b) Realized gain, and (c) Radiation efficiency.

GHz. The gap between successive unit cells is 2 mm to accommodate the PIN photodiodes.

Fig. 2 shows the numerical characterization of the unit-cell in terms of the refractive index (n) using CST Microwave Studio (MWS), which is an 3D electromagnetic solver [26]. It is evident from the figure the proposed unit-cell has a near zero refractive index (NZRI) over the entire frequency band of interest between 1.08 GHz and 1.48 GHz. The loss in the unit-cell is represented by the imaginary part of the refractive index shown in Fig. 2(b). It is found that the loss in the proposed antenna is much less than the loss of a single unit-cell. The reduction in the loss is attributed to the effects of coupling between the inner and outer rings of the unit-cell [27].

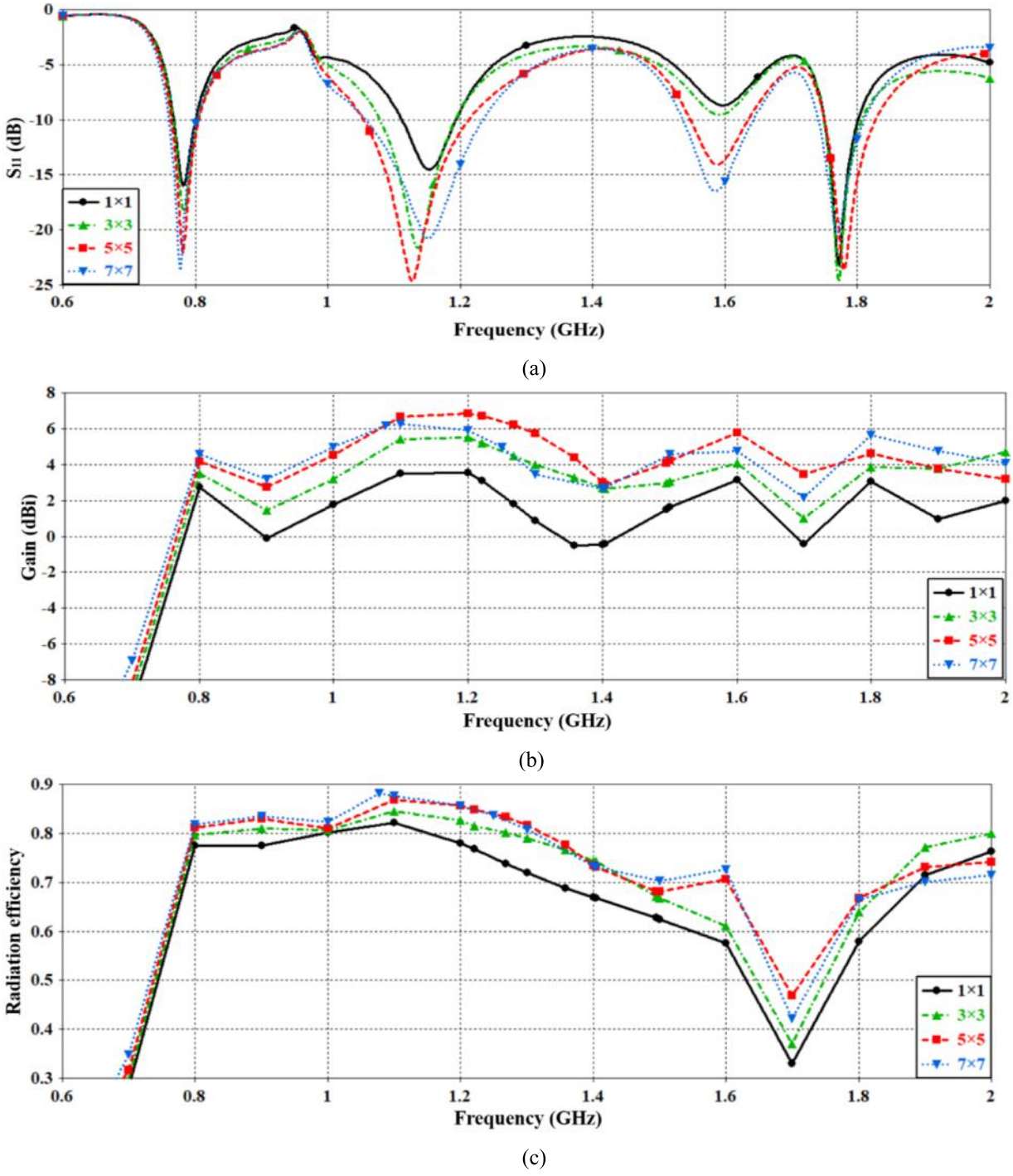

Fig. 6. Effect of metasurface matrix size on the antenna performance: (a) S_{11}, (b) realized gain, (c) radiation efficiency, and (d) F/B ratio.

3.2. Metasurface operation

Each metamaterial unit-cell has a certain electromagnetic aperture that acts like a spatial filter with a certain impulse response [28]. Therefore, the periodicity of the apertures constituting the metasurface layer can be represented by an impulse function. Consequently, the radiation pattern of the metasurface layer can be modeled by the periodic convolution function of the unit-cell (F_{uc}) when it's illuminated by incidence electromagnetic waves [28]. The overall radiation pattern of the metasurface layer (F_{SL}) can be evaluated using the following expression:

$$F_{SL} = F_{uc}\left[\frac{\mathrm{X}\sin(\pi v_x(N+1))}{\sin(\pi v_x X)}\right]\left[\frac{\mathrm{Y}\sin(\pi v_y(M+1))}{\sin(\pi v_y Y)}\right] \quad (1)$$

where, v_x and v_y are the periodicity along the *x*- and *y*-directions, respectively. *X* and *Y* are the interval displacements along the *x*- and *y*-directions, respectively. *N* and *M* represent the number of unit-cells in *x*- and *y*-directions. Since the proposed metasurface has an equal number of unit-cells in the *x*- and *y*-directions, Eqn.(1) simplifies to:

$$F_{SL} = F_{uc}\left[\frac{\mathrm{X}\sin(\pi v_x(N+1))}{\sin(\pi v_x X)}\right]^2 \quad (2)$$

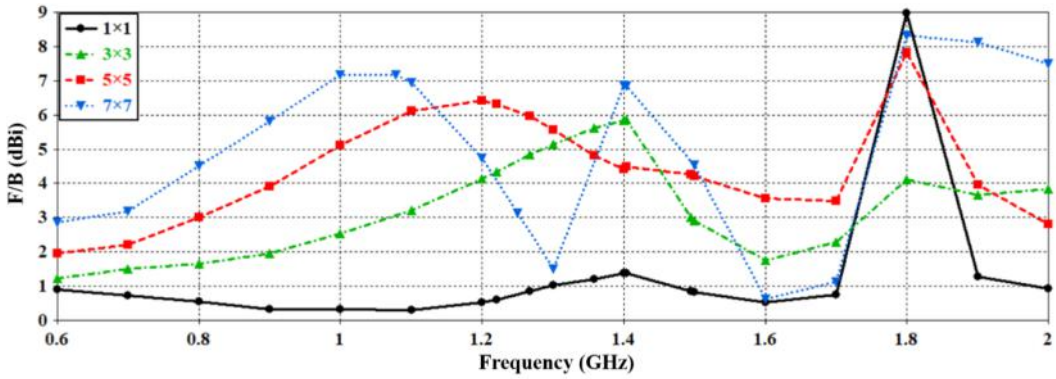

(d)

Fig. 6. (*continued*).

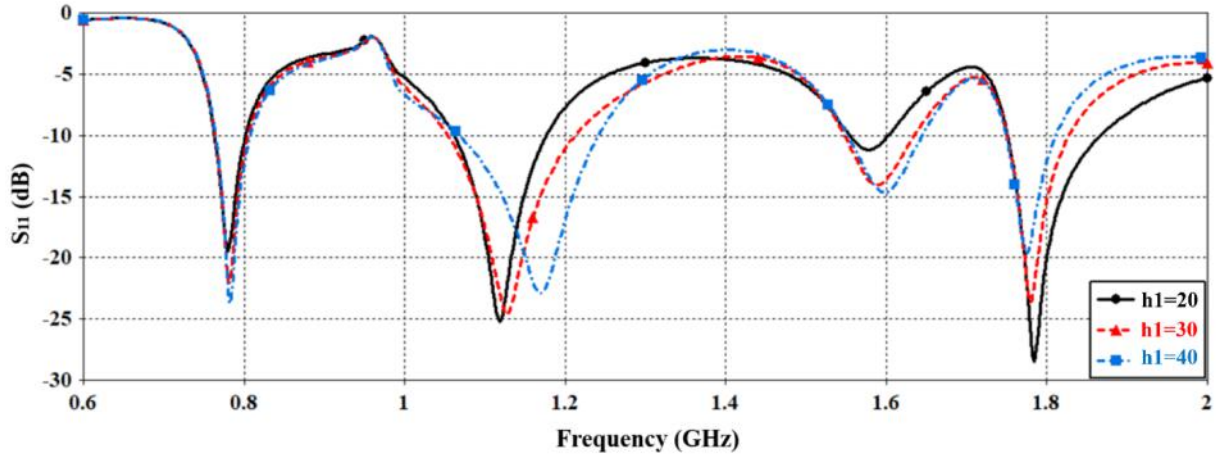

(a)

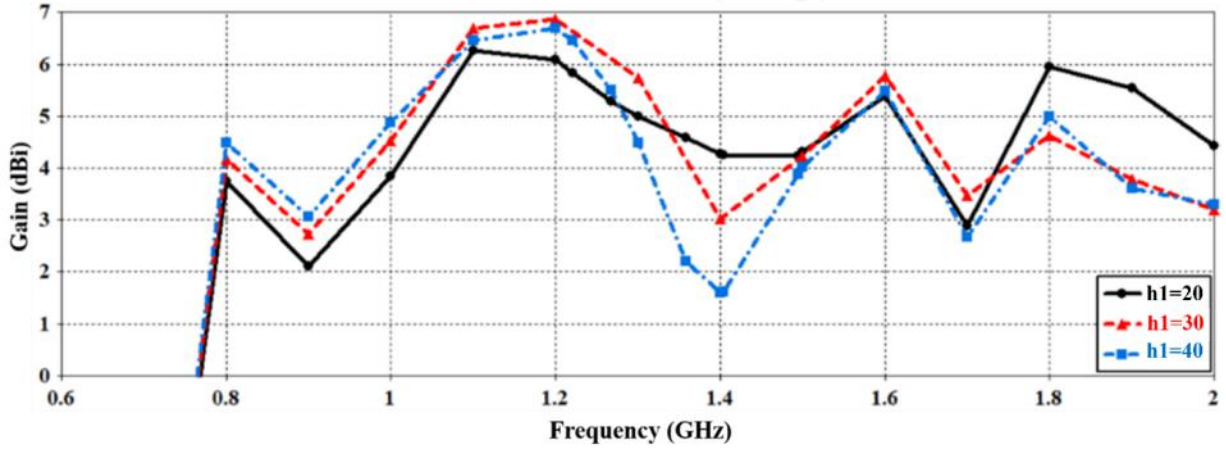

(b)

Fig. 7. Effect of metasurface spacing on the antenna performance: (a) S_{11}, and (b) Realize gain.

Since the unit-cell is small enough to be considered as an isotropic radiator, the value of F_{uc} is approximated to unity in all directions. Fig. 3 shows the exact value of F_{uc} pattern along the *x*- and *y*-directions evaluated using Eq. (2) and CST MWS. The accuracy of the theoretical expression is remarkable.

4. Antenna design methodology

4.1. Patch antenna design

The design of a standard rectangular patch antenna can be found abundantly in literature. The effective length and width are given by [20]:

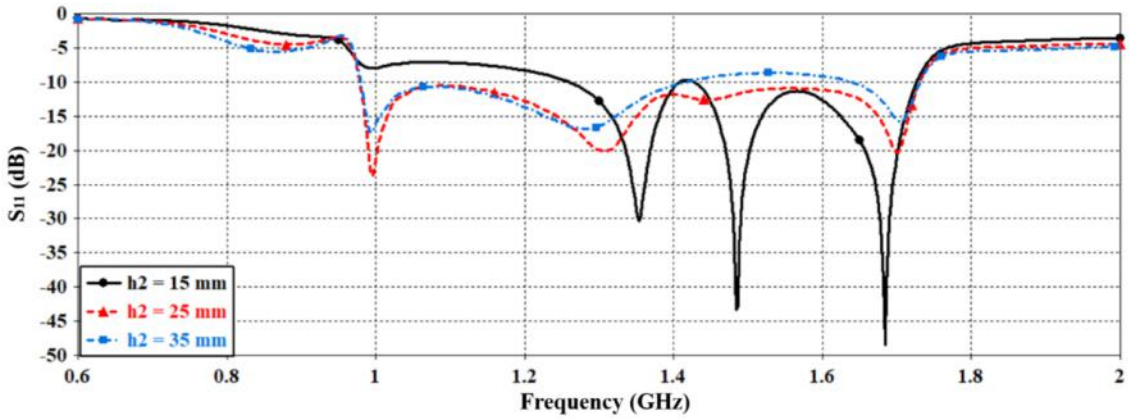

(a)

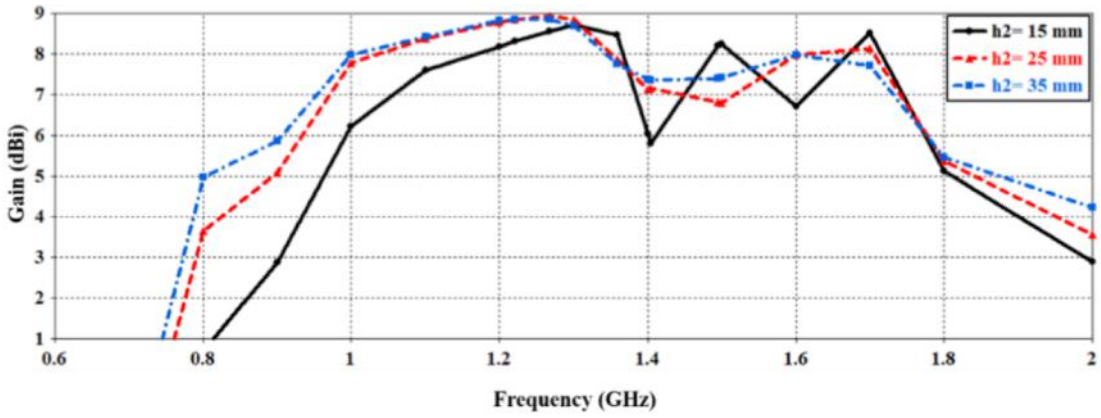

(b)

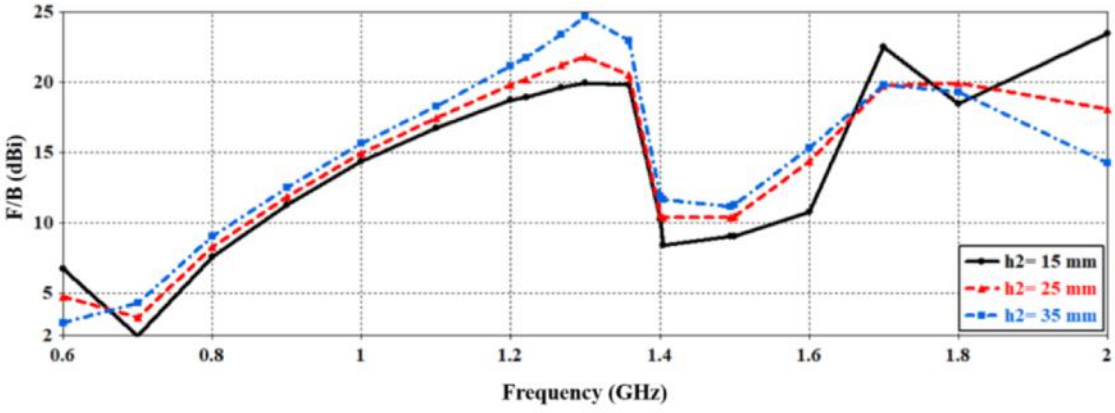

(c)

Fig. 8. Effect on reflector spacing on the antenna performance: (a) S_{11}, (b) realized gain, and (c) F/B ratio.

$$L = \frac{\lambda_o}{2\sqrt{\varepsilon_{eff}}} - \Delta \tag{3}$$

$$W = \frac{c}{2f_r}\left(\frac{\varepsilon_r + 1}{2}\right)^{-1/2} \tag{4}$$

where

$$\varepsilon_{eff} = \frac{\varepsilon_r + 1}{2} + \frac{\varepsilon_r - 1}{2}\left(1 + \frac{12h}{W}\right)^{-1/2}$$

$$\Delta l = 0.412h\left(\frac{\varepsilon_{eff} + 0.3}{\varepsilon_{eff} - 0.258}\right)\frac{(W/h) + 0.264}{(W/h) + 0.8}$$

The parameter W is the microstrip line width, h is the thickness of the substrate, ε_r is the dielectric constant of the substrate, ε_{eff} is the effective dielectric constant, and Δl is the correction term accounting for the fringe capacitance. The patch was embedded with H-tree shaped fractal slots of order 3. The feedline is a 50 Ω microstrip line.

4.1.1. *Fractal effect*

Fractals are geometric shapes that display self-similarity or repetition through the full range of scale [29]. Fractal have been applied in the design of multi-band and broadband microstrip [30]. In this paper, the H-tree shaped fractal slot is applied on the rectangular patch. The order of the fractal was determined by studying the effect of the fractal order on the antenna's reflection coefficient response, shown in Fig. 4. The 1st

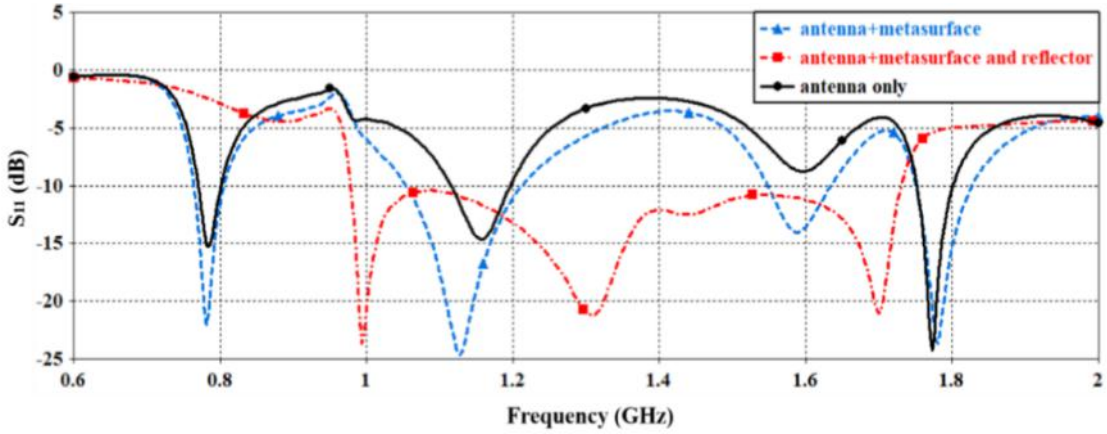

(a)

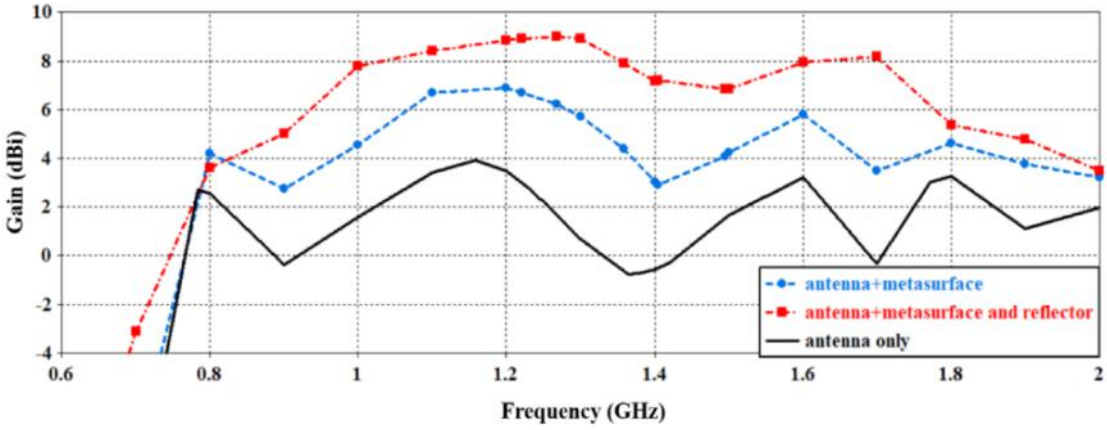

(b)

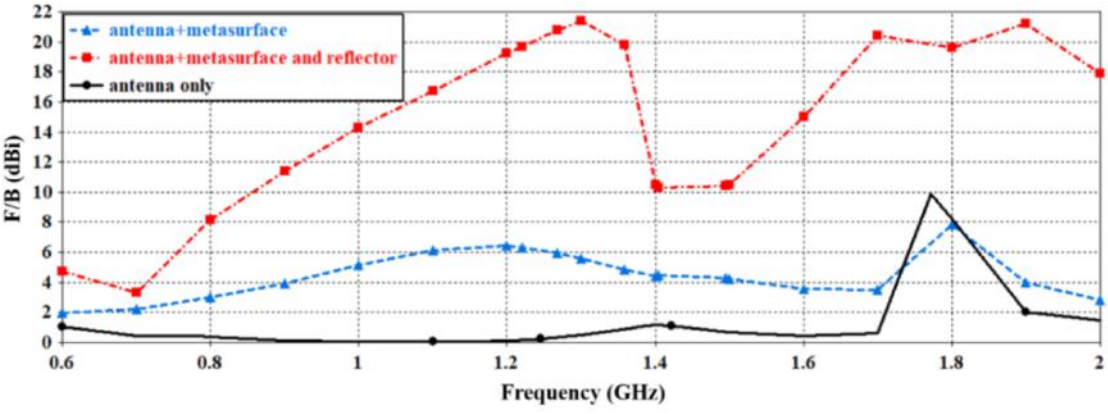

(c)

Fig. 9. The overall effect of including the metasurface layer in front of H-Tree fractal slot patch with a backside reflective surface: (a) S_{11}, (b) Realized gain, (c) F/B ratio, and (d) 3D radiation pattern.

order response shown in the green dot-dash curve has two resonant dips. The low dip at 0.75 GHz and a large dip where $S_{11} \leq -10$ dB at 1.57 GHz. The 2nd order has two dips for $S_{11} \leq -10$ dB at 0.87 GHz and at 1.77 GHz. The 3rd order has three dips for $S_{11} \leq -10$ dB at 1.17 GHz, 1.79 GHz and 1.975 GHz. It can be observed from the figure that a higher order fractal generates more resonance frequencies. This is attributed to the increased current paths.

4.1.2. Ground plane aperture effect

The effect of the ground plane aperture on the antenna's performance was investigated. The proposed antenna's ground plane was modified by etching a rectangular slot or aperture directly underneath the patch, as shown in Fig. 1(d). The results of the analysis in terms of S_{11}, gain, and radiation efficiency are shown in Fig. 5. It is evident from Fig. 5 that with the aperture the antenna's reflection coefficient, gain and radiation efficiency are significantly improved. The average gain between 0.8 GHz and 2 GHz without the aperture is −20 dBi, and with the aperture it is 2 dBi. The overall improvement obtained is 22 dBi. Over the same frequency range, the average improvement in efficiency is 70 %. This is because the aperture mitigates capacitive

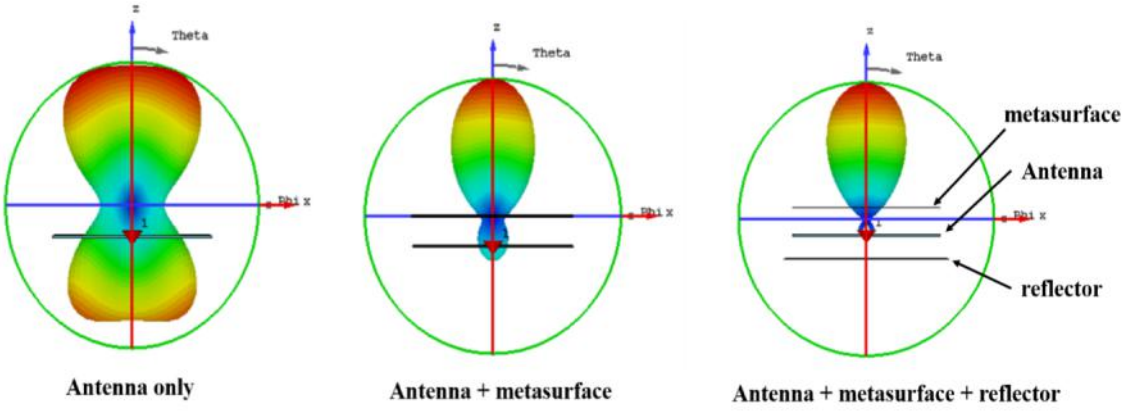

(d)

Fig. 9. (*continued*).

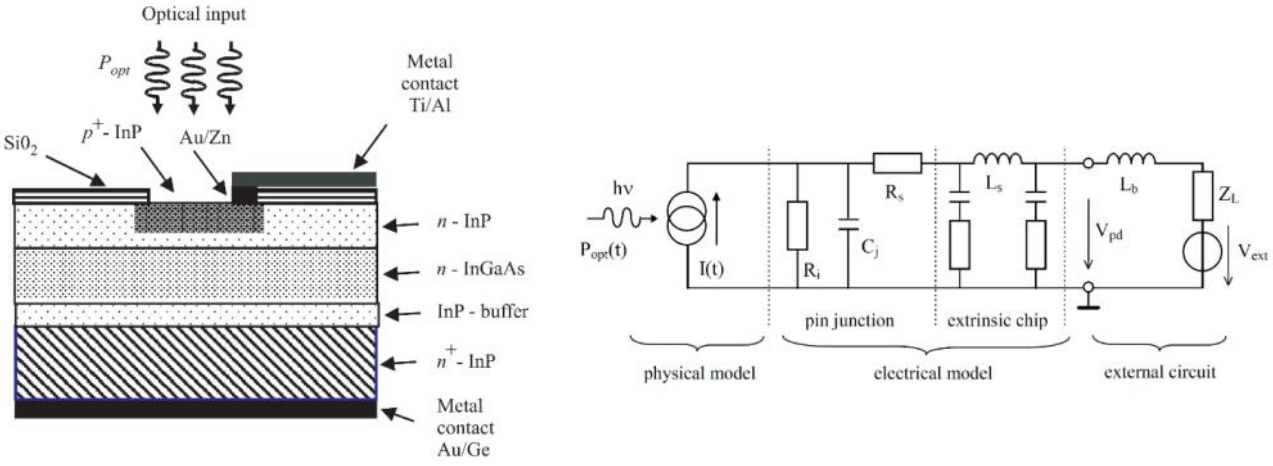

(a) (b)

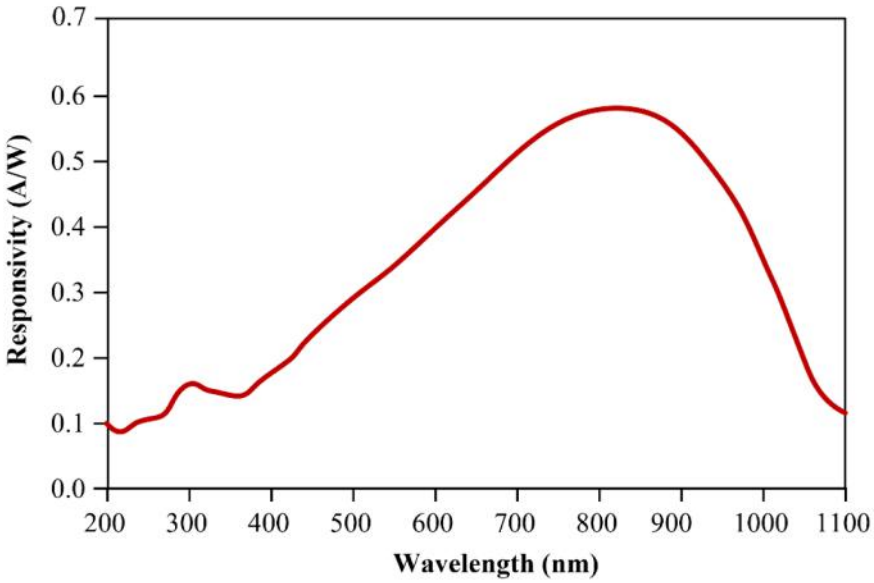

Fig. 10. (a) Cross section of the PIN photodiode structure, (b) Equivalent circuit of the PIN photodiode, and (c) Measured spectral responsivity of the PIN photodiode.

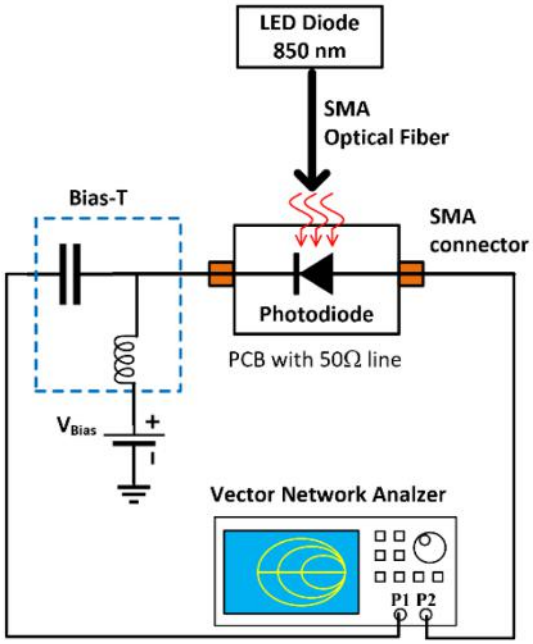

(a)

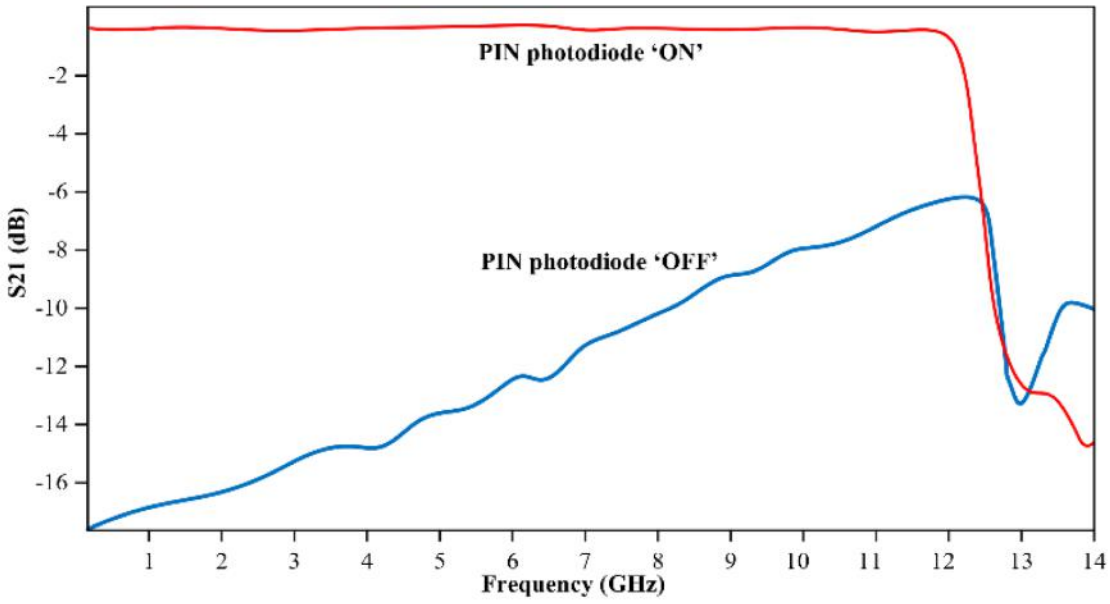

(b)

Fig. 11. (a) Setup and test fixtures to obtain the frequency response of the PIN photodiode switching response, and (b) Measured frequency response of the PIN photodiode in the 'On' and 'Off' state.

coupling between the patch slots and the ground plane that would otherwise trap some of the RF energy and undermine the antenna's gain and radiation efficiency.

4.2. Metasurface inclusion

The metasurface unit-cell employed here consists of two square rings where one of the rings is enclosed inside the other ring. The inner ring is offset by 45° with respect to the outer ring and its size is such that its corners touch the outer ring, as shown in Fig. 1(b). The purpose of the unit-cell is to present an NZRI medium to incident electromagnetic signals over a frequency range of interest. The NZRI surface has been shown to converge incident collimated electromagnetic waves [12,31]. This property is exploited here to increase the directivity of the proposed antenna.

When electromagnetic waves impinge on the metasurface layer the magnitude of the amplitude and phase of the wave at each unit-cell will differ [5]. The consequence of various metasurface sizes is investigated here. Also investigated here are the gap between the patch and the metasurface layer, and the gap between the patch and the reflective surface.

4.2.1. Metasurface matrix size

Effect of the metasurface size on its performance is studied here in

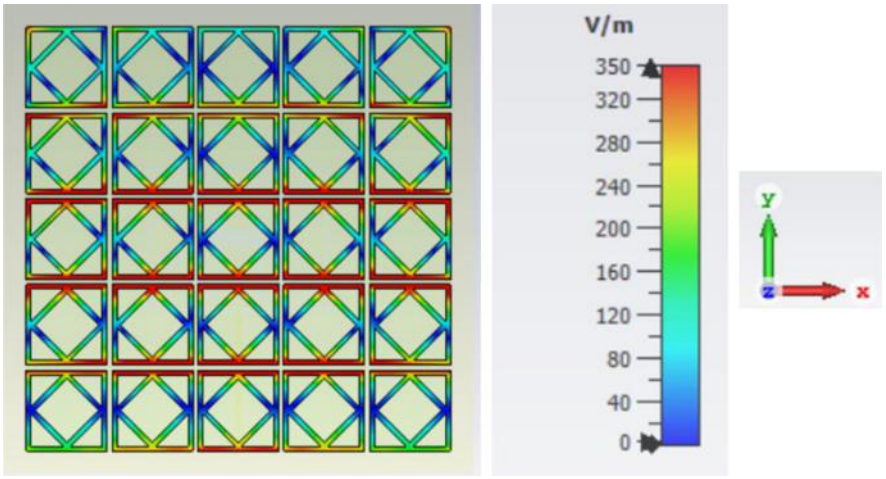

(a) State 1 - All PIN photodiodes switched off.

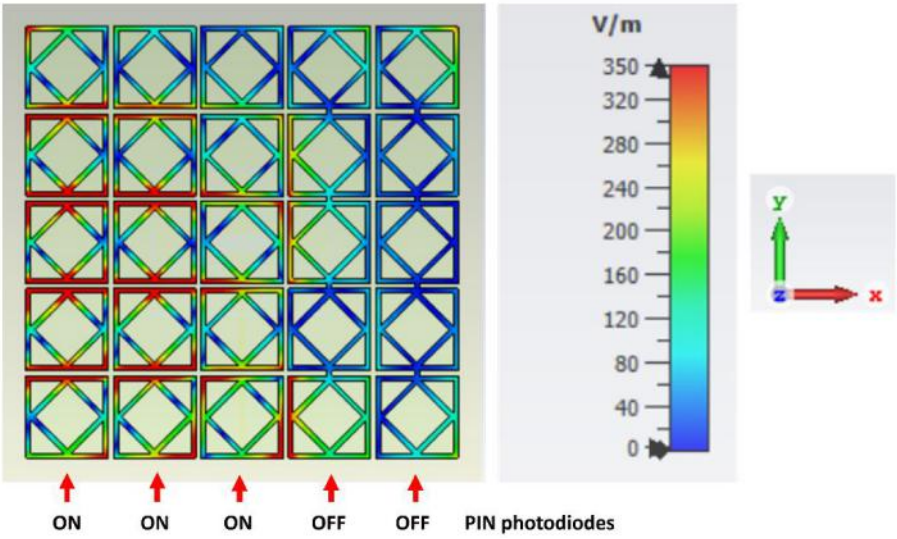

(b) State 2 - Columns #4 & #5 are switched off.

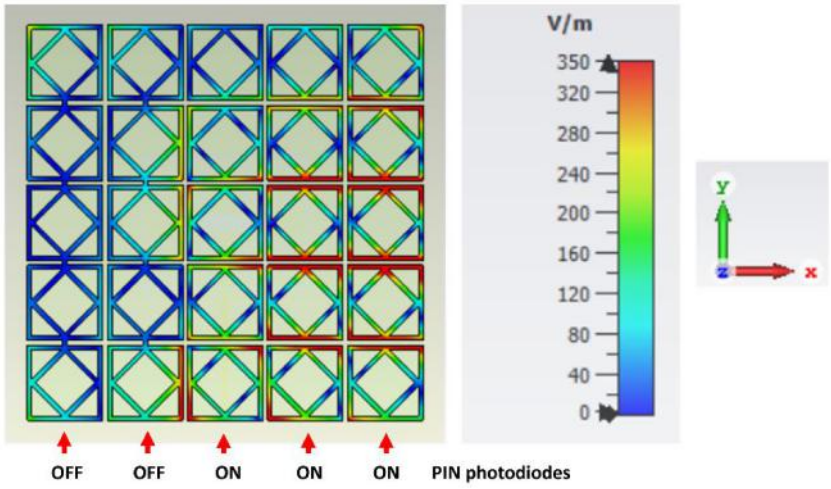

(c) State 3 - Columns #1 & #2 are switched off.

Fig. 12. Simulation result of the electric field distribution over the proposed antenna at 1.35 GHz for: (a) State 1, (b) State 2, and (c) State 3.

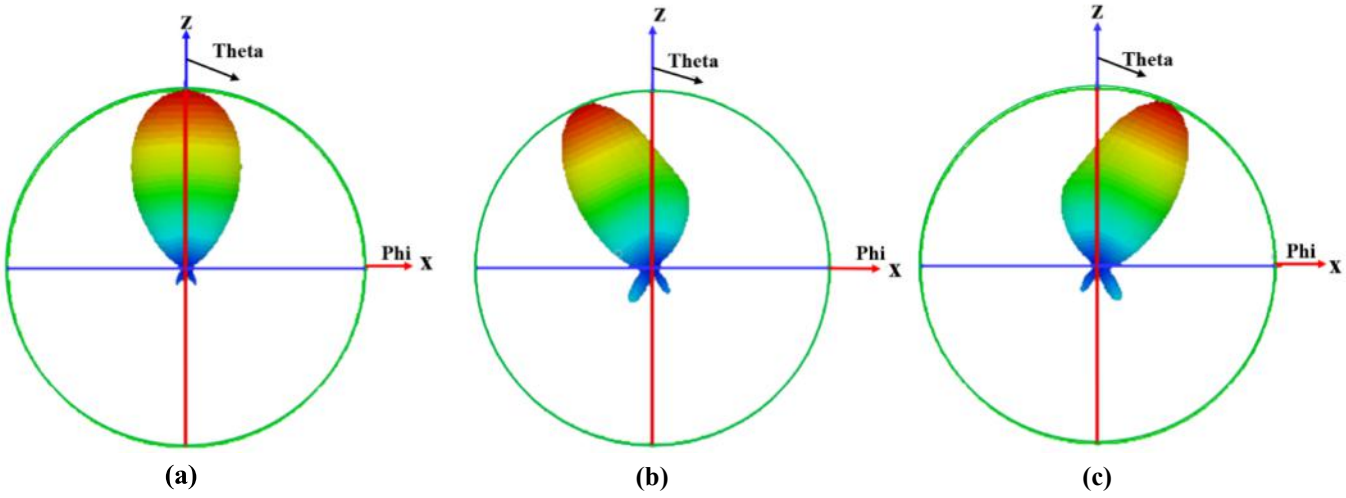

Fig. 13. Simulated radiation pattern of the proposed antenna at 1.35 GHz for: (a) State 1, (b) State 2, and (c) State 3.

Table 2
Operation states of the proposed antenna.

Deactivated columns	Main beam direction
–	0^o
#5	-20^o
#4 & #5	-24^o
#1	20^o
#1 & #2	24^o

terms of S_{11}, gain, radiation efficiency, and F/B ratio. Fig. 6(a) shows how the S_{11} response is affected by various matrix sizes, i.e., 1×1, 3×3, 5×5, 7×7. It is evident from this figure that the impedance matching (S_{11}) increases with a larger matrix size but in the case of the second response at 1.15 the impedance matching declines for matrix size higher than 5×5. Also, the impedance bandwidth of the second response increases with larger matrix size. The improvement in S_{11} is attributed to the effects of surface wave suppression with increasing the metasurface size [21]. The effect on the gain response is shown in Fig. 6(b). Over 0.7 GHz to 1.09 GHz the gain increases with larger matrix size however at frequencies above 1.09 GHz this is not the case. Matrix size greater than 5×5 does not enhance the gain performance between 1.09 GHz and 1.76 GHz. Fig. 6(c) shows the radiation efficiency increases with increase in matrix size over 0.7 GHz to 1.6 GHz, but this is not the case for frequencies above 1.6 GHz. The front-to-back ratio in Fig. 6(d) shows increase in matrix size improves the F/B ratio but this case applies between 0.6 GHz and 1.13 GHz and between 1.82 GHz and 2 GHz. From this analysis it is evident that the optimum matrix size is 5×5. As a result, this size was used in the proposed antenna.

4.2.2. *Metasurface spacing*

Air gap spacing between the metasurface and the antenna was investigated on the performance of the antenna. The gap spacing was varied from 20 mm to 40 mm in a step size of 10 mm. Fig. 7(a) shows the increase in the gap (h1) has no effect on the first S_{11} response at 0.78 GHz and marginal effect on the third response at 1.78 GHz. There is marginal effect on the second response at 1.12 GHz by gap size of 20 mm and 30 mm, however a gap of 40 mm shifts the center response from 1.13 to 1.17 GHz. Fig. 7(b) shows the gain changes by approximately 1 dB for different gap sizes. The gap of 30 mm provides higher gain between 1.1 GHz and 1.34 GHz and between 1.52 GHz and 1.73 GHz. The variation in the gain is attributed to the progressive phase variation across the metasurface. The gap spacing of 30 mm, which is about $\lambda/8$ at 1.13 GHz, was used in the design of the proposed antenna.

4.2.3. *Reflector effect*

The effect of the reflector spacing in Fig. 1(a) on the antenna's performance was also investigated. The purpose of the reflector was to block the radiation from the backside of the antenna and thereby enhance the front-to-back ratio. Fig. 8 shows how the spacing of the reflector had on S_{11}, gain and F/B ratio. It is evident that S_{11} improves with gap spacing of 25 mm and 35 mm. The graph in Fig. 8(a) shows that the optimum spacing for $S_{11} \leq -10$ dB is 25 mm across 0.99 GHz and 1.72 GHz. Fig. 8(b) shows the gain obtained is higher for spacing of 25 mm and 35 mm however the gain advantage between the two gap spacings is on average about 0.5 dBi. Fig. 8(c) shows the F/B ratio is higher for spacing of 35 mm from 0.68 GHz to 1.66 GHz however this is on average higher compared to 15 mm by 2.5 dBi. The reflector gap spacing used in the proposed antenna was 25 mm.

4.3. *3- overall performance comparison*

Fig. 9 shows there is significant improvement in the antenna's performance by stacking the metasurface layer above the patch and the conductive reflector below it with appropriate air gap spacing. Fig. 9(a) plots show extension in the impedance bandwidth for $S_{11} \leq -10$ dB is achieved between 0.978 GHz and 1.73 GHz which corresponds to a fractional bandwidth of 55.5 %. Over this frequency range the enhancement in gain is about 4 dBi and the average gain is about 7 dBi. Fig. 9(c) shows that over 0.978 GHz to 1.73 GHz the average F/B ratio improves by approximately 16 dBi and the average F/B ratio is 14 dBi. Fig. 9(d) shows by adding the metasurface and reflector layers the back lobe radiation is virtually eliminated and a highly directional radiation is realized.

5. Beam steering mechanism

The mechanism for steering the main beam radiated from the proposed antenna is achieved by switching 'On' and 'Off' a certain column of PIN photodiodes mounted on the metasurface layer shown in Fig. 1. The PIN photodiode chip used is based on InGaAs from QPHOTONICS (part no. DPDWM40-OM-FC/APC) which has a maximum operating frequency of 12 GHz. The cross section of the PIN photodiode is shown in Fig. 10(a). The PIN photodiode is composed of the physical and the electrical model parts. The electrical model of the PIN photodiode, shown in Fig. 10(b), consists of intrinsic chip model (junction capacitance, junction and series resistance), the extrinsic chip (e.g., bonding pad capacitance) and the external circuit, which is a 50 Ω load. Details on the model can be found in references [31–33]. The measure of the

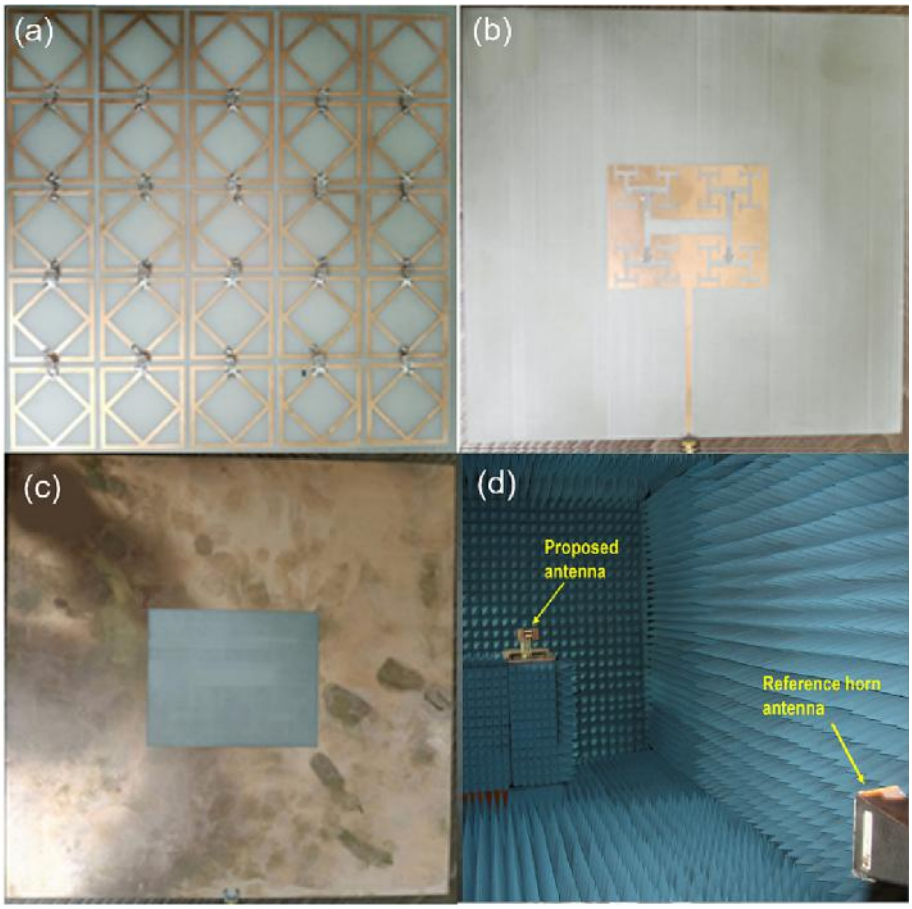

Fig. 14. Fabricated prototype of proposed antenna: (a) metasurface with PIN photodiodes, (b) front-view of the patch antenna, (c) back-view of the patch antenna, and (d) anechoic chamber with the measurement setup.

sensitivity to light, i.e., responsivity, of the photodiode is defined as the ratio of the photocurrent to the incident light power at a given wavelength. The measured responsivity in Fig. 10(c) shows the effectiveness of the photodiode in converting the light power into electrical current. The PIN diode has an optimum responsivity at a wavelength of 850 nm.

The experimental setup used to measure the frequency response of the 'On' and 'Off' state of the PIN photodiode is shown in Fig. 11(a). An LED of wavelength 850 nm was used to active and deactivate the photodiode. The Vector Network Analyzer used was Rohde & Schwarz R&S®ZNB. Fig. 11(b) shows the magnitude of the insertion-loss (S_{21}) as a function of frequency for the 'On' state (with applied light of wavelength 850 nm from LED) and 'Off' state (without applied light). The measured results show that the cut-off frequency of the photodiodes in the 'On' state is slightly above 12 GHz, which is consistent with information given by the manufacturer. In the 'On' state the insertion-loss is about −0.5 dB, and the 'Off' state the insertion-loss is greater than −16 dB in the desired frequency range of operation between 1 GHz and 2 GHz. In the 'Off' state the magnitude of S_{21} decreases with increase in frequency.

If we had used visible light containing different wavelength between 380 nm and 700 nm the insertion-loss performance would have been compromised. Visible light therefore was not an option for practical purposes.

By deactivating certain columns of photodiodes results in variations in the electric field distribution over the metasurface that effects the direction in which the main beam is firing. By strategically photonically controlling the activation and deactivation of the PIN photodiodes the direction of the main beam can be precisely controlled.

To gain a better understanding of how the electric field distribution over the metasurface layer changes, the antenna was modelled using CST MWS. Fig. 12(a) shows under state 1 when all the PIN photodiodes are switched 'Off' the electric field is most intense over unit-cell rows two to four. The superposition of the radiation from all unit-cells creates a directional broadside beam as shown in Fig. 13(a). In state 2, PIN photodiodes in columns #4 and #5 counting from the left-hand side are deactivated. Fig. 10(b) shows the resulting electric field intensity is concentrated mostly over the first three columns. This indicates phase coherence over these columns. The consequence if this is deflection of the beam by −24° in the elevation plane, as shown in Fig. 13. In state 3, when the left-hand side column #1 and #2 in Fig. 13(c) are deactivated, the electric field is concentrated over the right-hand side columns causing beam deflection of +24° in the elevation plane, as shown in Fig. 13. The total beam steering obtainable is 48°. These results are given in Table 2.

6. Results – design validation and discussion

Prototype of the fabricated antenna and the measurement set-up employed is shown in Fig. 14. The antenna was fabricated using the standard photolithography. This involves placing the mask of the antenna pattern on a substrate which has negative photoresist coated on it and exposing the entire structure to UV-light. The mask is then removed, and chemical etching is used to dissolve away the unexposed microstrip regions leaving behind the required circuit pattern. Photolithography was used to create the metasurface layer. The PIN photodiodes were soldered directly on the metasurface layer. The overall antenna was an assemblage of the three components, i.e., the metasurface layer, the patch antenna, and the reflective layer. Foam pillars were used to

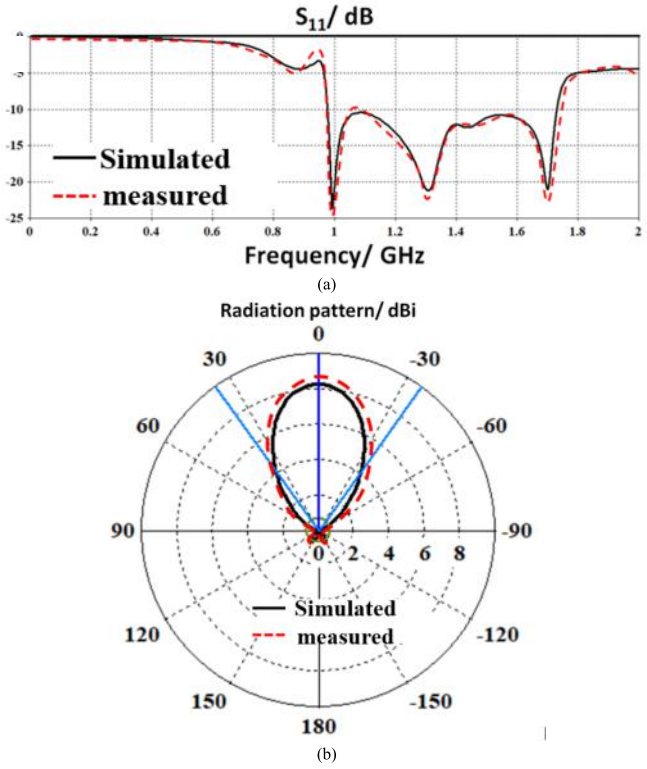

Fig. 15. Simulated and measured antenna characteristics for state 1 when all the PIN photodiodes are deactivated: (a) S_{11}, and (b) radiation pattern.

implement the required air gap between the patch and the two layers. The antenna was fed RF energy through an SMA connector. The radiation pattern of the proposed antenna was measured in a standard anechoic chamber [20].

Fig. 15 shows the simulated and measured antenna performance of the antenna in terms of S_{11} and radiation pattern. The measured results show that the proposed antenna has a fractional bandwidth of 55 % from 0.96 GHz to 1.78 GHz for $S_{11} \leq -10$ dB. The measured gain at the antenna's mid-band frequency of 1.35 GHz is approximately 9 dBi. The antenna radiates unidirectionally in the broadside when all the PIN photodiodes on the metasurface are deactivated. These results confirm the antenna is an excellent candidate for long range wireless communication systems.

The antenna's beam forming process was validated by activating and deactivating the metasurface PIN photodiodes under different scenarios. The PIN photodiodes used are sensitive to light of wavelength 850 nm. Under darkness the photoresistor presents a high electrical resistance. Conversely when photoresistor is exposed to light from a LED of 850 nm its electrical resistance significantly reduces. In fact, the magnitude of its resistance reduces rapidly with increase in light intensity. This is evident from the measurements shown in Fig. 11(b). This property is exploited here to control the performance of the metasurface layer. Under state 2 when the PIN photodiodes in columns #4 and #5 of Fig. 12(b) are deactivated the antenna's main beam deflects to the left by -24° in the elevation plane, as shown in Fig. 16(a). Under state 3 when the PIN photodiodes in columns #4 and #5 of Fig. 12(b) are deactivated the antenna's main beam deflects to the right by $+24^{\circ}$ in the elevation plane, as shown in Fig. 16(b). Other combinations of photonic illumination of the photoresistor provide different degrees of deflection. The maximum beam steering achievable with this technique is total 48°.

The proposed antenna whose radiation pattern can be controlled photonically is compared in Table 3 with other beam steering

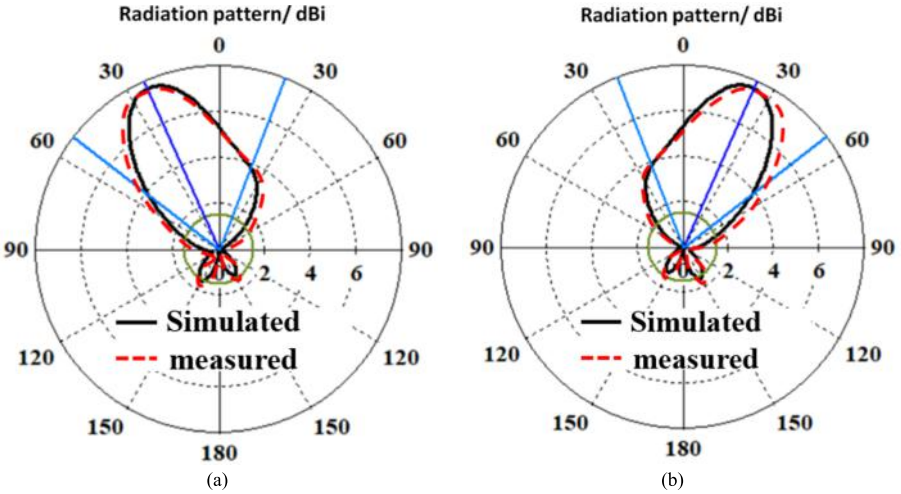

Fig. 16. Simulation and measured of radiation pattern at mid-band frequency of 1.35 GHz for: (a) state 2 when PIN photodiodes in columns #4 and #5 in Fig. 12 are deactivated, and (b) state 3 when PIN photodiodes in column #1 and #2 in Fig. 12 are deactivated.

Table 3
Comparison of the proposed antenna with pervious works.

Ref.	Fractional bandwidth	Dimensions	Max scan angle	Max gain (dBi)	Mechanism
[5]	30 %@1.05 GHz	$0.9\lambda_o \times 0.9\lambda_o \times 0.06\lambda_o$	$\pm 25^o$	9.4	PIN diodes
[31]	3.8 %@ 2.6 GHz	$1.04\lambda_o \times 1.04\lambda_o \times 0.06\lambda_o$	$\pm 20^o$	5.7	Fluid
[25]	27 %@0.92 GHz	$0.98\lambda_o \times 0.77\lambda_o \times 0.06\lambda_o$	$\pm 30^o$	8	PIN diodes
[13]	11.5 %@5.2 GHz	$1.16\lambda_o \times 1.16\lambda_o \times 0.26\lambda_o$	$\pm 36^o$	9.3	PIN diodes
[34]	4.1 %@5.5 GHz	$0.6\lambda_o \times 0.6\lambda_o \times 0.05\lambda_o$	$\pm 32^o$	7.2	Mechanically
[35]	2.77 %@3.6 GHz	$4.2\lambda_o \times 4.2\lambda_o \times 0.72\lambda_o$	$\pm 20^o$	13.9	Varactor diodes
[36]	10.6 %@9.41 GHz	$1.59\lambda_o \times 0.86\lambda_o \times 0.12\lambda_o$	$\pm 30^o$	5.11	MEMS switches
This work	55.5 %@1.35 GHz	$0.778\lambda_o \times 0.778\lambda_o \times 0.25\lambda_o$	$\pm 24^o$	9	PIN photodiodes

mechanisms reported recently in literature in terms of dimensions, maximum scan angle, and maximum gain. The dimensions and gain of the proposed antenna are comparable to other beam steering techniques however the proposed antenna offers beam steering in the elevation planes by a maximum of $\pm 24^{\circ}$. Unlike other methodologies reported to date the proposed technique uses light to affect beam steering. This novel technique mitigates the complexity and interference issues associated with other prior techniques.

7. Conclusion

Demonstrated for the first time is a novel reconfigurable metasurface antenna for beam steering applications in wireless communication systems. The antenna is designed to operate across 0.978 GHz to 1.73 GHz with a reflection-coefficient (S_{11}) better than -10 dB. The antenna comprises three layers. The middle layer is a rectangular patch antenna on which is implemented H-Tree shaped fractal slots. Located above the patch antenna is a metasurface layer consisting of a lattice structure constructed from unit-cells that are interconnected to each other by PIN photodiodes. The backside of the patch antenna is shielded with a reflective surface that ensures a high front-to-back ratio. The metasurface focuses the main beam emanating from the antenna to enhance its directivity. Surface currents over the metasurface can be perturbed by activating the PIN photodiodes when illuminated with LED light of wavelength 850 nm. It is shown that by activating appropriate PIN photodiodes on the metasurface the antenna's main beam can be controlled precisely. Maximum beam deflection achieved with the proposed mechanism is 48° from -24° to $+ 24^{\circ}$ in the elevation plane. The antenna offers a maximum gain of 9 dBi and its front-to-back ratio is 21 dBi at its mid-band frequency of 1.35 GHz. The antenna has a fractional bandwidth of 55.5 % from 0.978 GHz to 1.73 GHz. The antenna is low profile and compact with dimensions of $0.778\lambda_o \times 0.778\lambda_o \times 0.25\lambda_o$ mm^3. In the future, we plan to design flat antennas at other frequency bands where size and space are a constraint. In fact, the proposed technology is a applicable for use as intelligent and reprogrammable surface required for 6G mobile communication systems. This work can be extended in the development of smart antennas for future wireless systems operating at terahertz frequency band.

Declaration of Competing Interest

The authors declare that they have no known competing financial interests or personal relationships that could have appeared to influence the work reported in this paper.

Data availability

No data was used for the research described in the article.

Acknowledgments

Dr. Mohammad Alibakhshikenari acknowledges support from the CONEX-Plus programme funded by Universidad Carlos III de Madrid and the European Union's Horizon 2020 research and innovation programme under the Marie Sklodowska-Curie grant agreement No. 801538. The authors also sincerely appreciate funding from Researchers Supporting Project number (RSP2023R58), King Saud University, Riyadh, Saudi Arabia. Additionally, this work was supported by Ministerio de Ciencia, Innovación y Universidades, Gobierno de España (Agencia Estatal de Investigación, Fondo Europeo de Desarrollo Regional -FEDER-, European Union) under the research grant PID2021-127409OB-C31 CONDOR. Besides above, the Article Processing Charge (APC) was afforded by Universidad Carlos III de Madrid (Read & Publish Agreement CRUE-CSIC 2022).

Appendix A. Supplementary material

Supplementary data to this article can be found online at https://doi.org/10.1016/j.aeue.2023.154652.

References

[1] Kammoun A, Debbah M, Alouini M-S. Design of 5G full dimension massive MIMO systems. IEEE Trans Commun 2017;66(2):726–40.
[2] Karthika K, Kavitha K. Reconfigurable antennas for advanced wireless communications: A review. Wirel Pers Commun 2021;120(4):2711–71.
[3] Parchin NO, Jahanbakhsh Basherlou H, Al-Yasir YIA, Abd-Alhameed RA, Abdulkhaleq AM, Noras JM. Recent developments of reconfigurable antennas for current and future wireless communication systems. Electronics 2019;8(2):128.
[4] Kumar A, Kumar N, Dixit S. A Review on reconfigurable antennas for wireless communication systems. Turkish J Comput Math Educ 2021;12(14):348–66.
[5] Darvazehban A, Rezaeieh SA, Abbosh AM. Programmable metasurface antenna for electromagnetic torso scanning. IEEE Access 2020;8:166801–12.
[6] Qin C, Chen F-C, Xiang K-R-A. 5 x 8 butler matrix based on substrate integrated waveguide technology for millimeter-wave multibeam application. IEEE Antennas Wirel Propag Lett 2021.
[7] Ding C, Guo YJ, Qin P-Y, Yang Y. A compact microstrip phase shifter employing reconfigurable defected microstrip structure (RDMS) for phased array antennas. IEEE Trans Antennas Propag 2015;63(5):1985–96.
[8] Chou H-T, Yan Z-D. Parallel-plate Luneburg lens antenna for broadband multibeam radiation at millimeter-wave frequencies with design optimization. IEEE Trans Antennas Propag 2018;66(11):5794–804.
[9] Manoochehri O, Darvazehban A, Salari MA, Emadeddin A, Erricolo D. A parallel plate ultrawideband multibeam microwave lens antenna. IEEE Trans Antennas Propag 2018;66(9):4878–83.
[10] Darvazehban A, Manoochehri O, Salari MA, Dehkhoda P, Tavakoli A. Ultra-wideband scanning antenna array with Rotman lens. IEEE Trans Microw Theory Tech 2017;65(9):3435–42.
[11] Ji L-Y, Zhang Z-Y, Liu N-W. A two-dimensional beam-steering partially reflective surface (PRS) antenna using a reconfigurable FSS structure. IEEE Antennas Wirel Propag Lett 2019;18(6):1076–80.
[12] Hongnara T, Chaimool S, Akkaraekthalin P, Zhao Y. Design of compact beam-steering antennas using a metasurface formed by uniform square rings. IEEE Access 2018;6:9420–9.
[13] Cao YF, Zhang XY. A wideband beam-steerable slot antenna using artificial magnetic conductors with simple structure. IEEE Trans Antennas Propag 2018;66(4):1685–94.
[14] Ojaroudi Parchin N, Jahanbakhsh Basherlou H, Al-Yasir YIA, Abdulkhaleq M, Abd-Alhameed AR. Reconfigurable antennas: Switching techniques—A survey. Electronics 2020;9(2):336.
[15] Cao T, Hu T, Zhao Y. Research status and development trend of MEMS switches: A review. Micromachines 2020;11(7):694.
[16] Mavridou M, Feresidis AP. Dynamically reconfigurable high impedance and frequency selective metasurfaces using piezoelectric actuators. IEEE Trans Antennas Propag 2016;64(12):5190–7.
[17] Fakharian MM. A massive MIMO frame antenna with frequency agility and polarization diversity for LTE and 5G applications. Int J RF Microw Comput Eng 2021;31(10):e22823.
[18] Elwi TA. Remotely controlled reconfigurable antenna for modern 5G networks applications. Microw Opt Technol Lett 2021;63(8):2018–23.
[19] Abdelati R, Mohamed S, Benhmammouch O, Abdelkebir EL, Said AO. The behavior of a CPW-Fed miscrostrip hexagonal patch antenna with H-Tree Fractal slots. Rev Méditerranéenne des Télécommunications 2015;5(2).
[20] Balanis CA. Antenna theory: Analysis and design. John wiley & sons; 2015.
[21] Yang F, RahmatSamii Y. Electromagnetic band gap structures in antenna engineering. Cambridge UK: Cambridge university press; 2009.
[22] Elwi TA. Printed microwave metamaterial-antenna circuitries on nickel oxide polymerized palm fiber substrates. Sci Rep 2019;9(1):1–14.
[23] Asadpor L, Ghorbani T, Rezvani M. A compact multilayer wide-band and high-gain circularly polarized antenna. J Instrum 2018;13(10):P10003.
[24] Almizan H, Elwi TA, Hassain ZAA. Novel reconfigurable intelligent EBG Metasurface layer for ASK modulation. Res Square 2021. https://doi.org/10.21203/rs.3.rs-260100/v1.
[25] Darvazehban A, Rezaeieh SA, Zamani A, Abbosh AM. Pattern reconfigurable metasurface antenna for electromagnetic torso imaging. IEEE Trans Antennas Propag 2019;67(8):5453–62.
[26] CST Microwave Studio. [Online]. Available: http://www.cst.com.
[27] Pozar DM. Microwave engineering. John Wiley & sons 2011.
[28] Elwi TA, Al-Rizzo HM, Bouaynaya N, Hammood MM, Al-Naiemy Y. Theory of gain enhancement of UC-PBG antenna structures without invoking Maxwell's equations: An array signal processing approach. Prog Electromagn Res B 2011;34:15–30.
[29] Abdulkareem SF, Mezaal YS. Applications of fractal and quasi fractal geometries in slot antenna design: A review. J Mech Contin Math Sci 2019;14(4):216–38.
[30] Kumar G, Ghosh B, Chakrbarty S, Mahajan MB. Gain and bandwidth enhancement using NZRI–Metasurface. IETE J Res 2022:1–9.
[31] Naqvi AH, Lim S. A beam-steering antenna with a fluidically programmable metasurface. IEEE Trans Antennas Propag 2019;67(6):3704–11.

[32] Stolze A, Kompa G. Nonlinear Modelling of dispersive photodiodes based on frequency- and time-domain measurements. In: Proc. of the 26th EuMC, Prague, Czech Republic, Sept. 1996. p. 379–382.
[33] Chizh AL and Malyshev SA. Modeling and characterization of microwave p-i-n photodiode. In: Proc. Third Int. Conf. Adv. Semicond. Dev. Microsyst. (ASDAM'2000), Smolenice Castle, Slovakia, Oct. 2000. p. 239–242.
[34] Zhu HL, Cheung SW, Yuk TI. Mechanically pattern reconfigurable antenna using metasurface. IET Microwaves Antennas Propag 2015;9(12):1331–6.
[35] Reis JR, Vala M, Oliveira TE, Fernandes TR, Caldeirinha RFS. Metamaterial-inspired flat beamsteering antenna for 5G base stations at 3.6 GHz. Sensors 2021; 21(23):8116.
[36] Lago H, Zakaria Z, Jamlos MF, Soh PJ. A wideband reconfigurable folded planar dipole using MEMS and hybrid polymeric substrates. AEU-Int J Electron Commun 2019;99:347–53.

Zainab S. Muqdad received her B.Sc. degree in Electrical Engineering (2017) and her M. Sc. degree in Electronics and Communication Engineering (2022), both from the Mustansiriyah University, Baghdad, Iraq. Her research interests include antenna, microwave applications, microwave radiology imaging, neural network, metamaterials, biomedical wireless systems, and cancer detection.

Mohammad Alibakhshikenari was born in Mazandaran, Iran, in February 1988. He received the Ph.D. degree(Hons.) with European Label in electronicsengineering from the University of Rome "TorVergata'', Italy, in February 2020. He was a Ph.D. Visiting Researcher at the Chalmers University ofTechnology, Sweden, in 2018. His training duringthe Ph.D. included a research stage in the Swedishcompany Gap Waves AB. He is currently with theDepartment of Signal Theory and Communications, Universidad Carlos IIIde Madrid (uc3m), Spain, as the Principal Investigator of the CONEX (CONnecting EXcellence)-PlusTalent Training Program and Marie Skłodowska-Curie Actions. He was alsoa Lecturer of the electromagnetic fields and electromagnetic laboratorywith the Department of Signal Theory and Communications for academicyear 2021–2022 and he received the "Teaching Excellent Acknowledgement"Certificate for the course of electromagnetic fields from Vice-Rector ofstudies of uc3m. Now he is spending an industrial research period in SARAS Technology Limited Company, located in Leeds, United Kingdom, which is defined as his secondment plan by CONEX-Plus Program and Marie Skłodowska-Curie Actions. His researchinterests include electromagnetic systems, antennas and wave-propagations,metamaterials and metasurfaces, synthetic aperture radars (SAR), 5G and beyond wireless communications, multiple input multiple output (MIMO) systems, RFID tag antennas, substrate integrated waveguides (SIWs), impedance matching circuits, microwavecomponents, millimeter-waves and terahertz integrated circuits, gap waveguide technology, beamforming matrix, and reconfigurable intelligent surfaces (RIS), which led to achieve more than 4000 citations and H-index above 40 reported by Scopus, Google Scholar, and ResearchGate. He was a recipient of thethree years research grant funded by Universidad Carlos III de Madrid andthe European Union's Horizon 2020 Research and Innovation Program underthe Marie Skłodowska-Curie Grant started in July 2021, the two years research grantfunded by the University of Rome "Tor Vergata'' started in November 2019,the three years Ph.D. Scholarship funded by the University of Rome "TorVergata'' started in November 2016, and the two Young Engineer Awardsof the 47th and 48th European Microwave Conference were held in Nuremberg,Germany, in 2017, and in Madrid, Spain, in 2018, respectively. His research article entitled "High-Gain Metasurfacein Polyimide On-Chip Antenna Based on CRLH-TL for Sub TerahertzIntegrated Circuits'' published in Scientific Reports was awarded as the BestMonth Paper at the University of Bradford, U.K., in April 2020. He is servingas an Associate Editor for (i) *Radio Science*, and (ii) *IET Journal of Engineering*. He also acts as a referee in severalhighly reputed journals and international conferences.

Taha A. Elwi received his B.Sc. in Electrical Engineering Department (2003) (Highest Graduation Award), Postgraduate M.Sc. in Laser and Optoelectronics Engineering Department (2005) (Highest Graduation Award) from Nahrain University Baghdad, Iraq. From April 2005 to August 2007, he was working with Huawei Technologies Company, Baghdad, Iraq. On January, 2008, he joined the University of Arkansas at Little Rock and he obtained his Ph.D. in December 2011 from the system engineering and science. His research areas include wearable and implantable antennas for biomedical wireless systems, smart antennas, WiFi deployment, electromagnetic wave scattering by complex objects, design, modeling and testing of metamaterial structures for microwave applications, design and analysis of microstrip antennas for mobile radio systems, precipitation effects on terrestrial and satellite frequency re-use communication systems, effects of the complex media on electromagnetic propagation and GPS. The nano-scale structures in the entire electromagnetic spectrum are a part of his research interest.

Zaid Abedul Hassain was born in Baghdad (Iraq), in 1979. He received the B.Eng. degree in electrical engineering from University of Mustansiriyah, Baghdad, in 2000, and the master's degree in engineering science in 2002. He is currently a professor and the director of the antenna and microwave, department of Electrical Engineering, University of Mustansiriyah.

Bal S. Virdee (SM'08) received the B.Sc. and MPhil degrees in Communications-Engineering from the University of Leeds-UK and his Ph.D. in Electronic-Engineering from the University of London-UK. He has worked in industry for various companies including Philips (UK) as an R&D-engineer and at Teledyne Defence & Space (Shipley, UK) as a future products design engineer in RF/microwave communication systems. He has taught at several academic institutions in the UK before joining London Metropolitan University where he is a Senior Professor of Communications Technology in the School of Computing & Digital Media, and Director of the Center for Communications Technology. His research, in collaboration with industry and academia, is in microwave/millimeter-wave/terahertz wireless communications encompassing mobile-phones to satellite-technology. Prof. Virdee has chaired numerous technical sessions at IEEE international conferences and published numerous research papers. He is Chair and Executive Member of the Institution of Engineering and Technology (IET) Technical and Professional Network Committee on RF/Microwave-Technology. He is a Fellow of IET, a Chartered Engineer and a Senior-Member of IEEE. He is also a Senior Fellow of the Higher Education Academy.

Richa Sharma has over 20 years' experience in industry and academia, first as Network Engineer for Cisco Systems and then as Lecturer at Birmingham City University and London Metropolitan University. She completed her master's degree at Aston University. She is a qualified Cisco Certified Academy Instructor for CCNA and CCNP Courses internationally. Her research interests is on technology that drive social change and includes communications systems, metamaterials, IoT and artificial intelligence.

Nurhan Türker Tokan received her B.Sc. degree in Electronics and Communications Engineering from Kocaeli University in 2002 and her M.Sc. and Ph.D. degree in Communication Engineering from Yildiz Technical University (YTU), Istanbul, Turkey, in 2004 and 2009, respectively. From May 2003 to May 2009, she worked as a research assistant in the Electromagnetic Fields and Microwave Technique Section of the Electronics and Comm. Eng. Dept. of YTU, Istanbul, Turkey. Between May2 009 and April 2015, she worked as an assistant professor and between April 2015 and August 2021, she worked as an associate professor in the Electronics and Comm. Eng. Dept. of YTU. Since August 2020, she has been working as a professor at the same department. From October 2011 to October 2012, she was Postdoctoral researcher in the EEMCS Department of Delft University of Technology, Delft, Netherlands. From October 2012 to May 2013, she was a Postdoctoral Fellow supported by European Science Foundation at the Institute of Electronics and Telecommunications (IETR), University of Rennes1, Rennes, France. She is the author or coauthor of more than 50 papers published in peer-reviewed international journals and conference proceedings. Her current research interests are analysis and design of antennas with emphasis on dielectric lens antennas and wideband antennas, microwave circuits and intelligent systems.

Patrizia Livreri, (M'90) PhD, is a Professor with the Department of Engineering, University of Palermo, and a Visiting Professor with the San Diego State University. She received her "Laurea degree" in Electronics Engineering with honors in 1986 and her Ph.D. in Electronics and Communications Engineering in 1992, both from the University of Palermo, Italy. From 1993 to 1994, she was a researcher at CNR. Since 1995, she has been serving as the scientific director for the "Microwave Instruments and Measurements Lab" of the Engineering Department at the University of Palermo. In 2020, she also joined the CNIT National Laboratory for Radar and Surveillance Systems RaSS in Pisa. Her research interests are in microwave and millimeter vacuum high power (TWT, Klystron) and solid-state power amplifiers for radar applications; high power microwave source (virtual cathode oscillator, magnetically insulated transmission line oscillator); microwave and optical antennas, radar, and microwave quantum radar. She is the principal investigator of the "Microwave Quantum Radar" project, funded by the Ministry of Defense in 2021. She is the supervisor of many funded project and the author of more than 200 published papers.

Francisco Falcone (M'05, SM'09) received the degree in telecommunication engineering and the Ph.D. degree in communication engineering from the Universidad Pública de Navarra (UPNA), Spain, in 1999 and 2005, respectively. From February 1999 to April 2000, he was the Microwave Commissioning Engineer at Siemens-Italtel, deploying microwave access systems. From May 2000 to December 2008, he was a Radio Access Engineer at Telefónica Móviles, performing radio network planning and optimization tasks in mobile network deployment. In January 2009, as a co-founding member, he has been the Director of Tafco Metawireless, a spin-off company from UPNA, until May 2009. In parallel, he is an Assistant Lecturer with the Electrical and Electronic Engineering Department, UPNA, from February 2003 to May 2009. In June 2009, he becomes an Associate Professor with the EE Department, being the Department Head, from January 2012 to July 2018. From January 2018 to May 2018, he was a Visiting Professor with the Kuwait College of Science and Technology, Kuwait. He is also affiliated with the Institute for Smart Cities (ISC), UPNA, which hosts around 140 researchers. He is currently acting as the Head of the ICT Section. His research interests are related to computational electromagnetics applied to the analysis of complex electromagnetic scenarios, with a focus on the analysis, design, and implementation of heterogeneous wireless networks to enable context-aware environments. He has over 500 contributions in indexed international journals, book chapters, and conference contributions. He has been awarded the CST 2003 and CST 2005 Best Paper Award, the Ph.D. Award from the Colegio Oficial de Ingenieros de Telecomunicación (COIT), in 2006, the Doctoral Award UPNA, 2010, 1st Juan Gomez Peñalver Research Award from the Royal Academy of Engineering of Spain, in 2010, the XII Talgo Innovation Award 2012, the IEEE 2014 Best Paper Award, 2014, the ECSA-3 Best Paper Award, 2016, and the ECSA-4 Best Paper Award, 2017.

Ernesto Limiti (S'87–M'92–SM'17) is a full professor of Electronics in the Engineering Faculty of the University of Roma Tor Vergata since 2002, after being research and teaching assistant (since 1991) and associate professor (since 1998) in the same University. Ernesto Limiti represents University of Roma Tor Vergata in the governing body of the MECSA (Microwave Engineering Center for Space Applications), an inter-universitary center among several Italian Universities. He has been elected to represent the Industrial Engineering sector in the Academic Senate of the University for the period 2007-2010 and 2010-2013. Ernesto Limiti is actually the president of the Consortium "Advanced research and Engineering for Space", ARES, formed between the University and two companies. Further, he is actually the president of the Laurea and Laurea Magistrale degrees in Electronic Engineering of the University of Roma Tor Vergata. The research activity of Ernesto Limiti is focused on three main lines, all of them belonging to the microwave and millimetre-wave electronics research area. The first one is related to characterisation and modelling for active and passive microwave and millimetre-wave devices. Regarding active devices, the research line is oriented to the small-signal, noise and large signal modelling. Regarding passive devices, equivalent-circuit models have been developed for interacting discontinuities in microstrip, for typical MMIC passive components (MIM capacitors) and to waveguide/coplanar waveguide transitions analysis and design. For active devices, new methodologies have been developed for the noise characterisation and the subsequent modelling, and equivalent-circuit modelling strategies have been implemented both for small and large-signal operating regimes for GaAs, GaN, SiC, Si, InP MESFET/HEMT devices. The second line is related to design methodologies and characterisation methods for low noise circuits. The main focus is on cryogenic amplifiers and devices. Collaborations are currently ongoing with the major radioastronomy institutes all around Europe within the frame of FP6 and FP7 programmes (RadioNet). Finally, the third line is in the analysis methods for nonlinear microwave circuits. In this line, novel analysis methods (Spectral Balance) are developed, together with the stability analysis of the solutions making use of traditional (harmonic balance) approaches. The above research lines have produced more than 250 publications on refereed international journals and presentations within international conferences. Ernesto Limiti acts as a referee of international journals of the microwave and millimetre wave electronics sector and is in the steering committee of international conferences and workshops. He is actively involved in research activities with many research groups, both European and Italian, and he is in tight collaborations with high-tech italian (Selex - SI, Thales Alenia Space, Rheinmetall, Elettronica S.p.A., Space Engineering …) and foreign (OMMIC, Siemens, UMS, …) companies. He contributed, as a researcher and/or as unit responsible, to several National (PRIN MIUR, Madess CNR, Agenzia Spaziale Italiana) and international (ESPRIT COSMIC, Manpower, Edge, Special Action MEPI, ESA, EUROPA, Korrigan, RadioNet FP6 and FP7 …) projects. Regarding teaching activities, Ernesto Limiti teaches, over his istitutional duties in the frame of the Corso di Laurea Magistrale in Ingegneria Elettronica, "Elettronica per lo Spazio" within the Master Course in Sistemi Avanzati di Comunicazione e Navigazione Satellitare. He is a member of the committee of the PhD program in Telecommunications and Microelectronics at the University of Roma Tor Vergata, tutoring an average of four PhD candidates per year.